Activity of a Neuron and Synchronization in a Neural Group

Atsushi Fukasawa and Yumi Takizawa

***Abstract*—**This paper presents activity of a neuron and synchronization in a neural group.

Motion of electric charges is first presented at a boundary in electrolyte. A potential wall is formed by space charges and a depletion layer. Diffusion current is obtained across the boundary. An electro-physical modeling is given for a neuron with two depletion layers among three zones. An active neuron operates as an astable pulse generator.

Synchronization of a neural group is then presented to be realized by mutual pulse injection among neurons. Synchronization provides a neural system with common clock for high performance signal processing.

***Keywords*—**Activity of a neuron, electro-physical modeling, depletion layer, pulse generation, synchronization.

I. Introduction

RESEARCHES of biological neural systems have been studied in individual characteristics of kinds of neurons.

The research by the authors has been focused in characteristics common to kinds of neurons.

In this paper, an electro-physical modeling is assumed to study electro-physical dynamics estimated in a neuron.

A $p-n$ boundary is assumed in medium of electrolyte. The motions of charges are analyzed with diffusion equations. This leads to the result of modeling of electric diode between two zones. Then forming of a depletion layer and the potential wall at the boundary is shown by the analysis with the Poison's equation.

An electro-physical modeling is given for an active neuron with three zones and two depletion layers as a liquid active device. A neural group is then shown as a synchronous system realized by mutual pulse injection among neurons. Synchronous neural system provides a stable timing inside a neural group. The capability of recognition of events is produced by the time in common in a system of physical measures of time, space, and motion.

Manuscript received Sept 26, 2013: This work was supported in part by the Project of Transdisciplinary Research Integration Center on Human and Society system.

Atsushi Fukasawa was a Project Professor, the Institute of Statistical Mathematics. (e-mail: takizawa@ism.ac.jp)

Yumi Takizawa is an associate professor, the Institute of Statistical Mathematics, Tachikawa , Tokyo 190-8562, Japan (phone: 81-50-5533-8539; fax: 81-42-526-4335; e-mail: takizawa@ism.ac.jp).

II. Motion of Electric Charges at a Boundary in Electrolyte

A. Formation of electrical zones and a depletion layer

When electric charges are injected into a zone in electrical medium, charge density at the zone becomes higher and the other zone remains lower. It is assumed that quantity of injected charges is little and velocity of charges is low in the medium. A depletion layer is induced at a boundary between two zones.

Phase 1: Diffusion of charges by gradient of density F_D

Injected p-charges diffuse to n-zone, and n-charges diffuse to p-zone by the force of gradient of density F_D.

The operation is analyzed by the diffusion equation in II *B*.

Phase 2: Balance of diffusion F_D and Coulomb's force F_C

Coulomb's force FC (force by potential gradient) appears between diffused p- and n-ions. Directions of forces F_D and F_C are opposite. When they are balanced, diffusion is ceased.

The operation is analyzed by the Poison's equation in II *B*.

Phase 3: Cease of diffusion and formation of;
(a) p-zone and n-zone, and
(b) space charges and a depletion layer.

The charges included in a boundary are distributed at the edge of the boundary by the potential gradient (Coulomb's force) at the boundary.

A pair of space charges appears at both sides of the boundary.

Potential difference appears in the boundary. And electric charges are driven outside the boundary, and two zones and a depletion layer formed at the boundary.

The operation is analyzed by the equation in II *B*.

B. Diffusion current through a p–n boundary

p- and *n*- charges diffuse at a $p - n$ boundary by the gradient of density. Figure 1 shows *p*- and *n*-charge densities diffused by the gradients of their charge densities. A little amount of p_n and n_p exist in *n*- and *p*-regions as the minority charge under thermal equilibrium condition.

When electric charges are injected or dissipated in the medium, positive charge density $p(z)$ at point z is defined by Fick's diffusion equation with initial and boundary conditions.

$$-\frac{\partial p(z)}{\partial t} = -D_p \frac{\partial^2 p(z)}{\partial z^2} + \frac{p(z) - p_n}{\tau_p} \quad (1)$$

where, D_p (m^2/s) is diffusion coefficient. τ_p is diffusion lifetime of *p*-charges in *n*- region.

If the density changes slowly enough,

$$\partial p(z)/\partial t = 0 \quad (2)$$

$$\frac{d^2 p(z)}{dz^2} - \frac{p(z) - p_n}{D_p \tau_p} = 0 \quad (3)$$

The solution of Eq. (3) is given as;

$$p(z) - p_n = A\varepsilon^{z/L_p} + B\varepsilon^{-z/L_p} \quad (4)$$

$$L_p = \sqrt{D_p \tau_p} \quad (5)$$

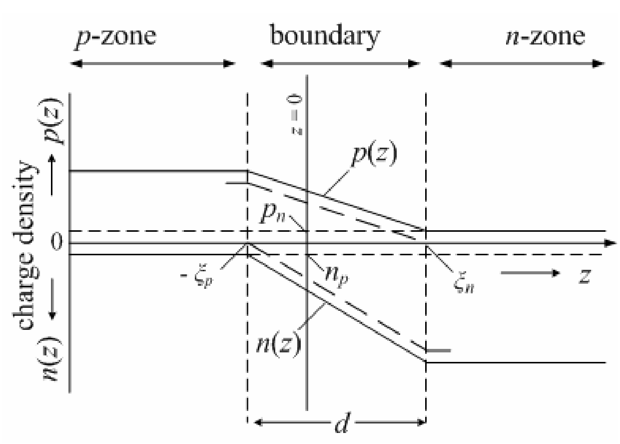

Fig. 1 Densities of *p*- and *n*-ions diffused with the gradients of charge densities.

The following conditions are given as;

$$\left.\begin{aligned} p(z) &= p_n \varepsilon^{-qV_B/kT} \;;\; z = 0 \\ p(z) &= p_n \;;\; z = \zeta_n \end{aligned}\right\} \quad (6)$$

where, $-V_B$ means a reverse bias. ζ_n is length of *n*-region.

The followings are obtained by substitituting Eq. (6) into (4).

$$A = \frac{p_n(1 - \varepsilon^{-qV_B/kT})\varepsilon^{-\zeta_n/L_p}}{2\sinh(\zeta_n/L_p)} \quad (7)$$

$$B = \frac{-p_n(1 - \varepsilon^{-qV_B/kT})\varepsilon^{\zeta_n/L_p}}{2\sinh(\zeta_n/L_p)} \quad (8)$$

Then,

$$p(z) = p_n\left\{1 - (1 - \varepsilon^{-qV_B/kT})\frac{\sinh\{(\zeta_n - z)/L_p}{\sinh(\zeta_n/L_p)}\right\} \quad (9)$$

The following is given by the differentiating Eq. (9),

$$\frac{dp(z)}{dz} = \frac{p_n(1 - \varepsilon^{-qV_B/kT})}{L_p}\frac{\cosh\{(\zeta_n - z)/L_p\}}{\sinh(\zeta_n/L_p)} \quad (10)$$

Current density J_p of *p*-charges at $z = 0$ is given as;

$$J_p = -q D_p \frac{dp(z)}{dz}$$

$$= \frac{q D_p p_n}{L_p}\frac{(\varepsilon^{-qV_B/kT} - 1)}{\tanh(\zeta_n/L_p)} \quad (11)$$

$$= \frac{q D_p p_n}{L_p}(\varepsilon^{-qV_B/kT} - 1) \;;\; \zeta_n >> L_p \quad (12)$$

Negative signs show decrease of density along time and *z*-axes. Charge density $n(z)$ of negative charges is also given as;

$$-\frac{\partial n(z)}{\partial t} = -D_n\frac{\partial^2 n(z)}{\partial z^2} + \frac{n(z) - n_p}{\tau_n} \quad (13)$$

τ_n is diffusion lifetime of *n*-charges in *p*- region.

Current density of *n*-charges J_n is also given as;

$$J_n = \frac{q\, D_n\, n_p}{L_n} (\varepsilon^{-qV_B / kT} - 1) \quad (14)$$

for the following condition.

$$\left.\begin{array}{ll} n(z) = n_p \varepsilon^{-qV_B/kT} & ;\ z = 0 \\ n(z) = n_p & ;\ z = \zeta_p \end{array}\right\} \quad (15)$$

Diffusion current *I* through the boundary with space *S* is given as the total of J_p and J_n which flow to apposite directions of *z*-axis.

$$I = q\ S\ (\frac{D_p p_n}{L_p} + \frac{D_n n_p}{L_n})(\ \varepsilon^{-qV_B / kT} - 1\ ) \quad (16)$$

$$= I_s\ (\ \varepsilon^{-qV_B / kT} - 1\ ) \quad (17)$$

$$I_s = q\ S\ (\frac{D_p p_n}{L_p} + \frac{D_n n_p}{L_n}) \quad (18)$$

where, I_s is saturation current.

C. Depth and Capacity of a Depletion Layer

Potential *V*(*z*) at a boundary is decided by true electric charge density $\rho(z)$ based on the Poison's equation.

$$\frac{d^2 V(z)}{dz^2} = -\frac{\rho(z)}{\varepsilon_e} \quad (19)$$

where, *z* is the longitudinal axis of a neuron, ε_e is the permittivity of electrolyte solution.

True electric charge is defined as the charge unrestrained to any place. Then polarization charge at the membrane is removed from $\rho(z)$, because the polarization charge is restrained to the membrane in a neuron.

True electric charge density $\rho(z)$ is given by the followings, and is shown in Fig.2 (a).

$$\left.\begin{array}{ll} \rho(z) = -q\ N_p & ;\quad -z_p \le z \le 0 \\ \rho(z) = +q\ N_n & ;\quad 0 \le z \le z_n \end{array}\right\} \quad (20)$$

where *Np*, *Nn* are true electric charge densities at *p*- and *n*-side of the boundary. *q* is elementary electric charge.

The electric field $dV(z)/dz$ is impressed at the boundary.

$$\left.\begin{array}{ll} \frac{dV_p(z)}{dz} = \frac{dV_n(z)}{dz} & ;\quad z = 0 \\ V_p(z) = V_n(z) & ;\quad z = 0 \end{array}\right\} \quad (21)$$

and,

$$\left.\begin{array}{ll} \frac{dV_p(z)}{dz} = 0 & ;\quad z = -z_p \\ \frac{dV_n(z)}{dz} = 0 & ;\quad z = z_n \end{array}\right\} \quad (22)$$

$\rho(z)$ is approximately zero outside the boundary.

$$\rho(z) = 0 \quad ; \quad z < -z_p, \quad z > z_n \quad (23)$$

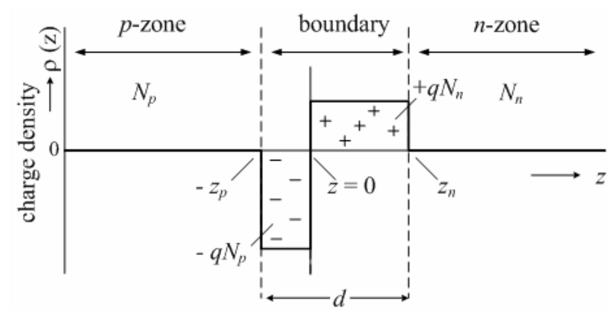

(a) Distribution of true electric charge density ρ(*z*).

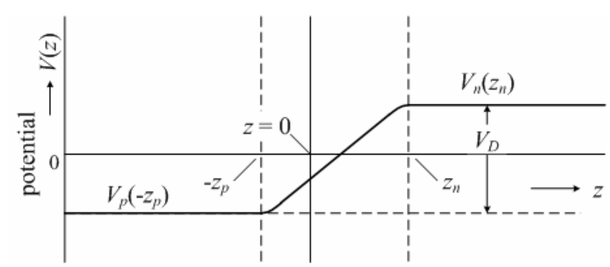

(b) Potentials *Vp*, *Vn*, and diffusion potential V_D .

Fig. 2 Distribution of true electric charge and diffusion potential of a boundary.

The potential $V(z)$ and the electric field $dV(z)/dz$ are continuous at $z = 0$. The following is obtained by solving Eq(19) and the conditions Eqs. (20) ~ (23).

$$N_p z_p = N_n z_n \tag{24}$$

It was proved that amount of *n*-charges at *p*- side is equal to the amount of *p*-charges at *n*- side of the boundary.

The potentials *Vp* and *Vn* are also obtained,

$$V_p = \frac{qN_p}{2\varepsilon_e} z^2 + \frac{qN_p z_p}{\varepsilon_e} z + B \tag{25}$$

$$V_n = -\frac{qN_n}{2\varepsilon_e} z^2 + \frac{qN_n z_n}{\varepsilon_e} z + B \tag{26}$$

The electrical diffusion potential V_D is defined as follows.

$$\begin{aligned} V_D &= V_n(z_n) - V_p(-z_p) \\ &= \frac{q}{2\varepsilon_e}(N_p z_p{}^2 + N_n z_n{}^2) \end{aligned} \tag{27}$$

The depth of depletion layer is given as,

$$\begin{aligned} d &= z_p + z_n \\ &= \left(\frac{2\varepsilon_e (N_p + N_n)}{qN_p N_n} V_D \right)^{\frac{1}{2}} \end{aligned} \tag{28}$$

Now, bias V_B is assumed applied to a boundary. When V_B is applied reversely to *n*-zone against *p*-zone, the depth of depletion layer d_B with reverse bias V_B is given as follows.

$$d_B = \left(\frac{2\varepsilon_e (N_p + N_n)}{qN_p N_n} (V_D + V_B) \right)^{\frac{1}{2}} \tag{29}$$

The positive charge Q per unit area at the boundary (*n*-side) is given as follows.

$$\begin{aligned} Q &= qN_n z_n = \left| -qN_p z_p \right| \\ &= \left(\frac{2\varepsilon_e q N_p N_n)}{N_p + N_n} (V_D + V_B) \right)^{\frac{1}{2}} \end{aligned} \tag{30}$$

The structure is assumed as an equivalent capacity.

$$c = \left| \frac{dQ}{dV} \right| = \left(\frac{\varepsilon_e}{2} \frac{qN_p N_n}{N_p + N_n} \frac{1}{V_D + V_B} \right)^{\frac{1}{2}} \tag{31}$$

When *VB* is applied forwardly at the boundary, the capacity is given changing V_B to $-V_B$.

III. Electro-Physical Modeling of a Neuron

A. Depth and capacity of depletion layers in a neuron

1) Whole aspects of a neuron

A neuron is exhibited as a three-port bio-electrical device with dendrite, central part, and axon terminal. These ports are assigned as input, ground, and output ports. The ends of dendrite and axon terminal are composed of multiple branches which are connected to previous and post neurons with synapses. Biochemical and electrical couplings are formed by synapses. A bio-electrical modeling is given in Fig. 3. An excitatory synapse is shown in the figure.

2) Signal p-ion injection to a resting neuron

During a neuron is resting, inner potential is kept negative and uniform inside the neuron. When neurotransmitters are released from previous neurons and accepted by the neuron, *p*-charges of Na^{+} are injected into the dendrite. Injected *p*-ions play as an excitatory signal into the neuron.

3) Motion of signal p-ions at the first depletion layer

The first depletion layer is formed between the dendrite and the central parts.

The depth d_1 and the equivalent input capacity c_d are given as;

$$d_1 = \left\{ \frac{2\varepsilon_e \ (N_d + N_{c1})}{q \ N_d \ N_{c1}} (V_{D1} - V_{B1}) \right\}^{\frac{1}{2}} \tag{32}$$

$$c_d = \left(\frac{\varepsilon_e}{2} \frac{qN_d N_{c1}}{N_d + N_{c1}} \frac{1}{V_{D1} - V_{B1}} \right)^{\frac{1}{2}} \tag{33}$$

where, N_d, N_{c1} are true electric charge density at the dendrite and input end of the central part.

V_{D1} V_{B1} are diffusion potential and bias appeared forwardly at the first depletion layer.

The depth d_1 becomes narrower as injected *p*-ion at the dendrite and/or the forward-bias V_B increases. Then signal *p*-ions pass over the first depletion layer easily.

4) *p*-ion injection to the axon terminal

A part of signal *p*-ions pass through the second depletion layer by the thermal motions. Ca channels inject *p*-ions (Ca^{2+}) inside the neuron by stimuli of arrived signal *p*-ions (Na+). The potential in this zone is enhanced, and the axon terminal forms *p*-zone covered by negative potential inside the neuron. By Ca^{2+} injection, charge allocation at the second depletion layer should be inverted as shown in Fig. 4. This configuration is defined by reverse diode with reverse bias voltage (refer to Fig.6).

5) Motion of signal *p*-ions at the second depletion layer

The second depletion layer is formed between the central part and the axon terminal. The depth d_2 and the equivalent output capacity c_a are given as;

$$d_2 = \left\{ \frac{2\varepsilon_e \, (N_{c2} + N_a)}{q \, N_{c2} \, N_a} (V_{D2} + V_{B2}) \right\}^{\frac{1}{2}} \qquad (34)$$

$$c_a = \left(\frac{\varepsilon_e}{2} \frac{qN_{c2}N_a}{N_{c2} + N_a} \frac{1}{V_{D2} + V_{B2}} \right)^{\frac{1}{2}} \qquad (35)$$

where, $Nc2$ and Na are true electric charge density at the dendrite and input end of the central part. V_{D2} V_{B2} are diffusion potential and bias appeared at the second depletion layer.

The depth d_2 becomes wider than depth d_1.

Signal *p*-ions pass over the second depletion layer by the force of thermal motion of ions.

6) Motion of induced signal *n*-ions

When signal *p*-ions arrive at the axon terminal, *n*-ions are injected into the axon terminal by Cl channels.

n-ions move from the right to the left passing over the second and then the first depletion layers. The motion of *n*-ions from right to left is forward, and from left to right is reverse.

These *n*-ions play also as the signal together with signal *p*-ions. The *p*- and *n*-ions carry signals to the same direction with the principle of duality.

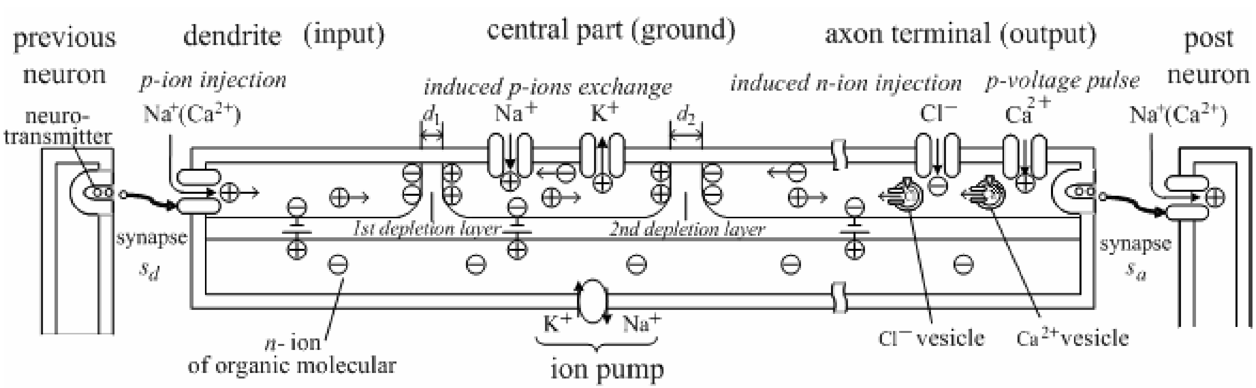

Fig. 3 Bio-electric modeling of an activated neuron. Leakage channels are abbreviated.

B. Energy Diagram of Electrical Charges

Energy of p- and n-ions in a neuron are illustrated in Fig. 4. The energy of *p*- and *n*-ions are assumed with a small difference to Fermi level as shown in the figure.

Cl channels at the axon terminal inject *n*-ions to left at the second depletion layer passing over a slope shown in the figure.

The duality of motions of *p*- and *n*-ions is well informed by tracing the curve to right (*p*-ion) and to left (*n*-ion). The three port configuration is kept in spite with a slope at the axon terminal (refer to [2]).

IV. Electrical Modeling of activity of a neuron

A. Electrical Activity in a Neuron

Electrical modeling of an active neuron is shown in Fig. 5.

i_d is the current of *p*-ions injected in the dendrite, i_a is the current of sum of arrived *p*-ions and *n*-ions injected by Cl-channels at the axon terminal. i_c is the current through resistance R_c of the central part to the outside of a neuron.

α is current multiplication factor and $\alpha \cdot i_d$ is equivalent current source for the axon terminal.

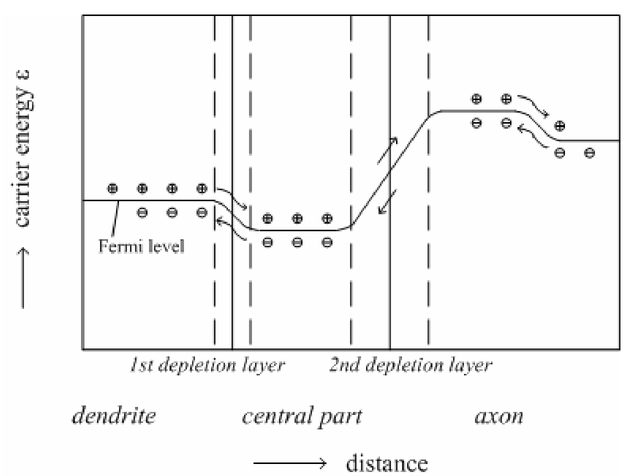

Fig. 4 Energy diagram of negative and positive ions with Cl⁻ channels at the axon terminal.

B. Characteristics as an Amplifier

Electrical modeling of an operating neuron is shown in Fig.6.

The points of d_0, a_0 are outside of membrane. c_0 is a virtual point taken in the central part. r_d and r_a are resistances of forward diode n_d and reverse diode n_a, r_c is the resistance at the central part to outside of a neuron. R_d and R_a are external resistances of synapses s_d and s_a.

$r_d << R_d$ and $r_a << R_a$. r_c is approximately zero. The capacities C_d and C_a are caused by the first and second depletion layers respectively. Input and output synapses s_d and s_a.are shown as forward diodes for excitatory synapses (*p*-ions). These synapses work as backward diodes for inhibitory synapses (*n*-ions).

Voltage amplification gain G is given as;

$$G = \frac{v_a}{v_d} = \frac{\dfrac{\alpha R_a}{r_d + r_c}}{1 - \dfrac{\alpha R_a}{r_d + r_c} \cdot \dfrac{r_c}{R_a}} = \frac{K}{1 - K\beta} \quad (36)$$

$$K = \alpha \frac{R_a}{r_d + r_c} \quad (37)$$

$$\beta = \frac{r_c}{R_a} \quad (38)$$

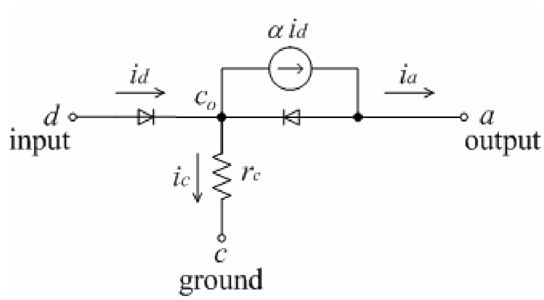

Fig. 5 Electrical modeling of an active neuron.

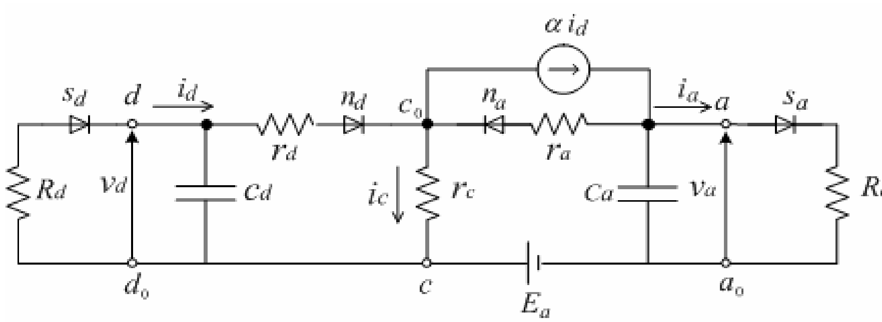

Fig. 6 Electrical modeling of an operating neuron.

where, v_d and v_a are input and output voltages of a neuron, G, K, β are closed loop gain, open loop gain, and inner feedback ratio of a neuron respectively. Oscillation condition is given by $K\beta \geq 1$.

In case that the axon terminal has little Cl channels, $\alpha < 1$, $K\beta << 1$. Therefore a neuron operates as an amplifier with threshold for input signal with positive inner feedback.

C. Characteristics as a Pulse Generator

The neuron operates as an oscillator to generate pulses when the product of open loop gain K and feedback ration β exceeds 1.

This oscillator is composed by self injection without input trigger.

$$T_1 = C_d \frac{r_c R_a}{r_c + R_a} \tag{39}$$

$$T_2 = C_a R_a \tag{40}$$

where, $R_d + r_d >> r_c$, $r_a = \infty$ are assumed for simplified analysis.

The period of oscillation T is given as the total time length as following;

$$T = T_1 + T_2 = C_d \frac{r_c R_a}{r_c + R_a} + C_a R_a \tag{41}$$

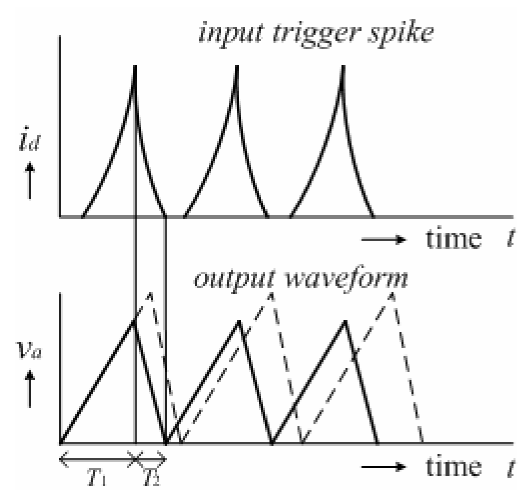

Fig. 7 Astable pulse generator with external injection. Dotted line is an original waveform. Solid line is a synchronized waveform to input trigger pulse.

D. Timing of Output Pulses

An oscillator operates in free running condition without external input. Timing of output pulse is adjusted in pull-in condition when external input i_d is added.

Output pulses v_a under free-running and pulled-in conditions are shown with dotted and solid lines in Fig. 8 respectively.

V. Organization of a Synchronous Neural System

A. System Synchronization of a neural group

Actual formulation of a neural group is given in Fig. 8. A small circle represents a neuron. Input and output signals of a neuron are at a branch of the dendrite and at a branch of the axon terminal. A set of pair neurons is shown in Fig. 8 (a). Connection between two neurons is performed by arrows with dual directions. A system of four neurons is shown in Fig.8 (b).

The timing of output pulse of an oscillator is adjusted by the other. When two oscillators are connected with each other, the timing is set at a certain timing between two. As number of oscillators increases, the variation of timings among neurons is reduced and system synchronization is established.

B. Synchronous Signal processing

This formulation enables system synchronization and synchronized signal processing simultaneously. Signal processing for multiple inputs and multiple outputs are available for dynamic processing including correlation, comparison, and detecting variations. This formulation will be required for complex, reliable, and fast operation and signal processing [6].

Appendix

A. Membrane model by Hodgikin-Huxley

Conventional model was ever given by Hodgkin and Huxley[7], and is popular even now.

This model was composed by the assumption that the membrane plays an essential roll of activity. Input *p*-charge at the dendrite induces polarization on the surface of the membrane and transmitted to the central part, where Na channel takes *p*-charges inside. These charges are transmitted through narrow cross section and amplified at the hillock.

The electrical circuit is shown by a condenser C_M and three resistances R_{Na}, R_K, and R_L with electric cells E_{Na}, E_K, and E_L for Na, K, and leakage channels.

1) Active element is not included.

This circuit is a certain circuit for charge – discharge operation. This circuit does not include any negative resistance nor other active elements. This circuit does not belong to any active circuit.

2) Membrane cannot transmit electric signal.

The potential and current to transmit information signal are defined by the true electric charge density and polarization charge on the membrane must be deleted from the true electric charge density as shown in Chapter 2 in this paper.

Electric communication system and computer are fist developed by inventions of three-port active devices (triode and transistor), and these actual systems could not composed only by two-terminal active devices.

(a) A set of two neurons. (b) A system by four neurons.

Fig. 8 Synchronization and signal processing by mutual injection.

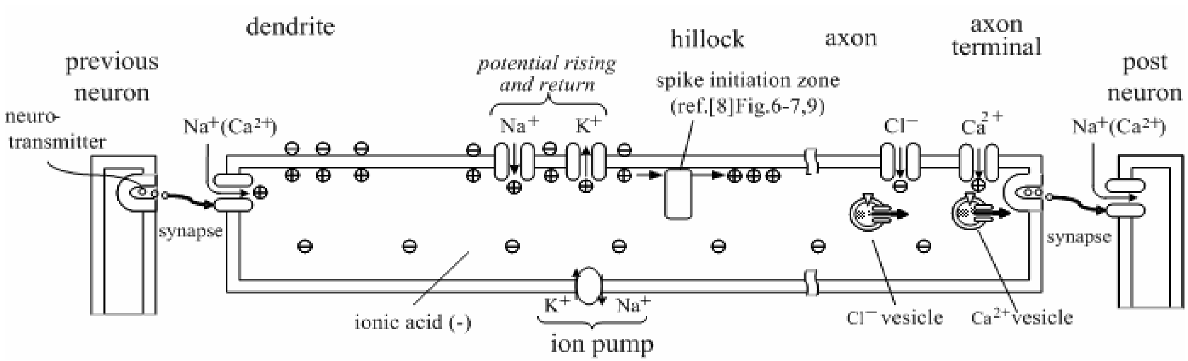

Fig. 9 Membrane model of an active neuron.

.

ACKNOWLEDGMENT

The authors express sincere gratitude for Professor Tomoyuki Higuchi, director-general, and Professor Hiroe Tsubaki, vice director-general, and Professor Noboru Sonehara, project leader of System of Human and Society for their leaderships and kind supports for this research.

The grater part of this study is supported by the project of Function and Induction with the Research Organization of Information and Systems.

The authors also express sincere gratitude for Professor Toshiharu Horie, Chiba University, Professor Kazuhiko Natori,, Toho University, and Professor Yoshikazu Miyanaga, Hokkaido University for their helpful advices.

REFERENCES

[1] Y. Takizawa, G. Rose, M. Kawasaki, "Resolving Competing Theories for Control of the Jamming Avoidance Response: The Role of Amplitude Modulations in Electric Organ Discharge Decelerations," Journal of Exp. Biol. 202, pp. 1377-1386, 1999.

[2] W. Shockley, “Electrons and holes in semiconductors,” D. Van, Nostrand, New York, 1950.

[3] K. Yanagisawa, “Transistor and its electric circuit,” (Japanese) Kyoritsu ,Tokyo, Dec. 1955.

[4] A. Fukasawa, “Active electric circuit and its application to antenna system, - Low noise amplifier with Esaki Diode,” Master Thesis of Waseda Univ., Apr.. 1966.

[5] A. Fukasawa, Y. Takizawa, “Activity of a Neuron and Formulation of a Neural Group for Synchronization and Signal Processing,” the Best Paper Award on NEUROLOGY’12, Proc. of the Int. Conf. on Neurology, pp.242-247, Kos, Greece, July 2012.

[6] Y. Takizawa, A. Fukasawa, “Signal Processing by a Neural System and its Application to Location of Multiple Events,” Int. Jour. of Applied Mathematics and Informatics, Vol. 6, Issue 3, pp. 126-133, 2012.

[7] A. L. Hodgkin, A. F. Huxley, “A quantitative description of membrane current and its application to conduction and excitation in nerve,” Bulletin of Mathematical Biology, Vol. 52, No. 1/2, pp.25-71, 1990.

[8] F. Delcomyn, “Foundations of neurobiology,” Freeman and co., New York, 1998.

[9] B. Hille, “Ion Channels of Excitable Membranes, 3rd ed.” Sinauer Associates, Ma., USA, 2001.

[10] A. Fukasawa, Y. Takizawa, “Activity of a Neuron and Formulation of a Synchronous Neural System,” Proc. of the Int. Conf. on Mathematical Methods, Computational Techniques, and Intelligent Systems, pp. 66-73, Mar. 21, 2013.

[11] A. Fukasawa, Y. Takizawa, “Activity of a Neuron and Formulation of a Neural Group,” Proc. of the Int. Conf. on Neurology’13, pp. 94-103, Chania, Greece, Aug. 27, 2013.

[12] Y. Takizawa, A. Fukasawa, “Knowledge on Events in Time, Space, and Motion with a Synchronous Neural System,” Proc. of the Int. Conf. on Neurology’13, pp. 104-109, Chania, Greece, Aug. 27, 2013.

Atsushi Fukasawa received the B.S. degree in Electrical Engineering from Chiba Unversity in 1962. He received the Master of Arts degree in Electrical communication from Waseda University, Tokyo, in 1967 and the Ph.D. degree from Waseda University in 1983.

He joined Graduate University of Science and Technology, Chiba University as a professor in 1997. He joined the department of Electrical and Electronics Engineering, faculty of Engineering, Chiba University in 1998, and the department of Urban Environmental and System Engineering, Chiba University in 1999. He joined Transdisciplinary Research Integration Center, Research Organization of Information and Systems as a project professor in 2004.

He received the Award of the Ministry if Science and Technology, Japan in 1967, and received the Ohm Science and Technology Prize from Ohmsha in 1994 respectively. He received also the Prize on Telecommunication System Technology from the Foundation of Telecommunication Association, Japan in 2004.

And he is also received WSEAS/NAUN the Best Paper Award of NEUROLOGY, 2012.

He is a senior member of the IEEE.

Yumi Takizawa received the B.S. degree in Physics from Shinshu University, Japan, in 1984, and the Ph.D. degree from the University of Tokyo in 1994. She was a research leader of signal processing for communication system Lab., OKI Electric Industry Co. Ltd., Tokyo since 1984. She joined the Institute of Statistical Mathematics, Japan as an associate professor in 1995.

She has been engaged nonstationary signal processing methods and its application to wide areas of industrial systems. She also has been engaged in digital mobile communication system of Wideband CDMA. Then she has been engaged in neuroethology of weakly electric fish as a visiting researcher at University of Virginia, 1997-1998 and 1999-2000. She continued research of biological signal processing including behavior of neural systems.

She received the Prize on Telecommunication System Technology from the Foundation of Telecommunication Association, Japan in 2004. She is an associate Professor.